Available online at www.sciencedirect.com

ScienceDirect

Green Energy & Environment 8 (2023) 1308e1324

www.keaipublishing.com/gee

Review article

High surface area biocarbon monoliths for methane storage

Elizabeth Michaelis [a], Renfeng Nie [b,*], Douglas Austin [a], Yanfeng Yue [a,*]

[a] Department of Chemistry, Delaware State University, Dover, DE 19901, United States
[b] College of Chemical Engineering, Zhengzhou University, Zhengzhou, Henan, 450001, China

Received 4 April 2022; revised 14 July 2022; accepted 21 July 2022
Available online 5 August 2022

Abstract

New energy sources that reduce the volume of harmful gases such as SO_x and NO_x released into the atmosphere are in constant development. Natural gas, primarily made up of methane, is being widely used as one reliable energy source for heating and electricity generation due to its high combustion value. Currently, natural gas accounts for a large portion of electricity generation and chemical feedstock in manufacturing plastics and other commercially important organic chemicals. In the near future, natural gas will be widely used as a fuel for vehicles. Therefore, a practical storage device for its storage and transportation is very beneficial to the deployment of natural gas as an energy source for new technologies. In this tutorial review, biomaterials-based carbon monoliths (CMs), one kind of carbonaceous material, was reviewed as an adsorbent for natural gas (methane) adsorption and storage.

Keywords: Activated carbon; Carbon monolith; Methane storage; High surface area; Activation agent

1. Introduction

Natural gas, composed of roughly 90% methane [1], has been used as a reliable energy source to power vehicles, houses, and heating systems. The over reliance on petroleum-based fuels for transportation raises concerns about the sustainability of oil reserves and the impact of greenhouse gas emissions [2]. Natural gas is less harmful to the ecosystem than other fossil fuels typically used for energy. Therefore, natural gas holds the potential of lowering pollution emissions, especially in urban areas with a high density of vehicles [3].

The transportation and storage of methane gas has been among the most significant barriers to its utilization. Currently, methane is primarily stored as compressed natural gas (CNG) and transported in a liquefied state [4]. However, CNG requires expensive vessels with multi-stage compression, and tanks are relatively heavy. Methane stored as liquefied natural gas (LNG) also requires expensive cryogenic processes. As an attractive alternative, adsorbed natural gas (ANG) for methane storage is considered a better choice for applications than CNG and LNG because ANG offers a higher volume to volume storage capacity than CNG, along with the advantage of a lower storage pressure [5–7]. Due to the aforementioned reasons, ANG is utilized in some vehicles by storing natural gas with adsorbents inside a vessel [8]. Therefore, for commercial applications of natural gas, the manufacturing of high adsorption capacity microporous adsorbents, such as low-cost carbonaceous adsorbents, is needed [9,10].

With the push for carbonaceous and bio carbonaceous adsorbents as a storage medium for natural gas, the precursor materials need to be readily available, low-cost, and naturally abundant. Many carbonaceous adsorbents are explored in literature, including powder-activated carbons, compressed activated carbons, aerogel carbons, carbon fibers, and carbon monoliths (CMs) [11–15]. These all have unique densities, surface areas, and microporosities that affect methane adsorption capacity and adsorption rate. Among these carbon

* Corresponding authors.
E-mail addresses: rnie@zzu.edu.cn (R. Nie), yyue@desu.edu (Y. Yue).

https://doi.org/10.1016/j.gee.2022.07.005

materials, CMs are attractive because they typically have the desired shape and morphology with tunable composition, structure, and porosity [16–20]. Monoliths are also advantageous, as blocks are easily handled and are more facile for installation, implementation, and cycling than activated carbon powders. A monolith still needs to be developed that meets all the needed parameters of large surface area, good microporosity, and high density, so further research is needed. In addition, once monolith methane adsorption is improved, the monolith still needs to perform in an application situation while maintaining a long life of adsorption and desorption cycles. This review will discuss the synthesis of CMs and their applications for natural gas/methane adsorption and storage. This review will focus on how different parameters in the synthesis of CMs affect methane uptake. Finally, the pros and cons of CMs, the future research directions for CMs, and the prospects for CM applications are also discussed.

2. Carbon monoliths

The ideal structure for monolith implementation into storage devices and vehicles is a solid block structure instead of loose powder [21]. Typically, CMs are formed by pressing activated carbon in a mold under high pressure or temperature, resulting in a continuous monolithic structure. Monoliths are typically discs shaped with a smaller height to diameter ratio. However, that is not always true; some are cylindrical, and some are in larger-scale rectangular demonstration block form. Also, the addition of honeycomb or circular channels in the monolith increases the overall surface area. As a gas adsorbent, CMs have several advantages compared to the powder carbon materials: (i) higher strength and better mechanical properties due to the monolithic shape, (ii) lower cost for recovery after use, and (iii) lower pressure drop when high flow rates are used because of the widespread parallel channels extending through the monolith body. Monoliths can have tailored textural and composition properties suitable for their particular application [22].

An optimal CM is necessary for the application of methane adsorption, as the Department of Energy requirements are 263 V/V volumetrically with a gravimetric loading, in the range of 0.27–0.56 kg kg^{-1} [11]. To achieve a high methane adsorption capacity, CMs often need to be synthesized to possess high density. In addition, introducing extra pores will increase the surface area, resulting in a high adsorption capacity. For instance, honeycomb structures fabricated in a monolith will benefit the gas adsorption capacity [16].

2.1. The preparation of carbon monoliths

The formation of activated CMs uses two main methods: binder or binder-less. Both methods utilize either high temperature or high pressure to form a monolith morphology. Additionally, a template can be used to create extra porosity as the template is removed after carbonization. The resulting activated carbon can then be formed into a monolith structure with a binder. Commonly, the activated carbon is mixed with a binder, resulting in a slurry, and then heated and pressed for a specific time in a mold. Finally, the binder will be carbonized under an inert atmosphere, resulting in a high-density carbon

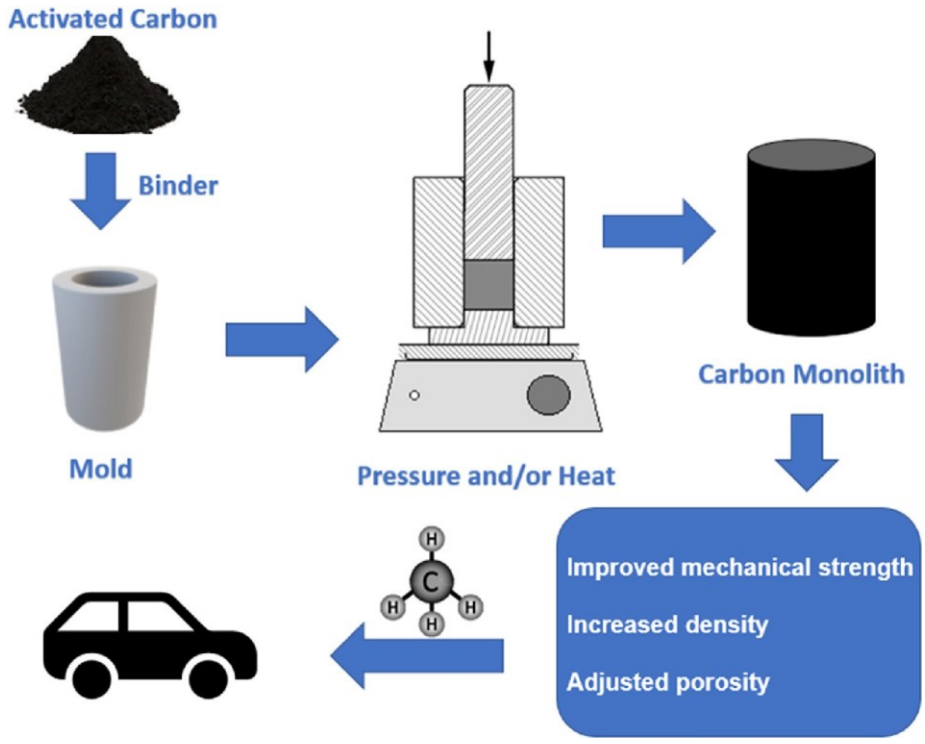

Scheme 1. Monolith formation process from activated carbon, to increase the mechanical strength and density.

adsorbent monolith (Scheme 1) [23–26]. Based on different applications, many kinds of CMs have been prepared by employing different molds, temperatures, and pressures (Fig. 1).

Lozano–Castelló and co-workers prepared activated CMs based on an activated carbon powder and multiple binders using conventional methods [27]. Their study showed that the methane adsorption capacity of these monoliths strongly depended on the material density and was also related to the adsorption ability of the starting activated carbon [27]. Rash and co-workers synthesized and characterized a new low pressure, monolithic, activated biocarbon adsorbent for methane storage from wood sawdust–derived activated carbon. This activated carbon was mixed with a binder in a rock tumbler with ball bearings for processing. This innovative process yielded a material whose gas adsorption performance was superior to metal–organic hybrid materials and other activated carbons, as a result of large tank volumetric and gravimetric storage capacities with rapid adsorption/desorption.

Compaction of activated carbon has also been done. This method is when only pressure is used to form a disc shape without the addition of a binder or heat. This is not the same as monolith formation, as the compaction method does not achieve the same solid structure as monoliths. On top of that, the compression has led to pore collapses, so there was no way to further increase the pore development of these structures [28].

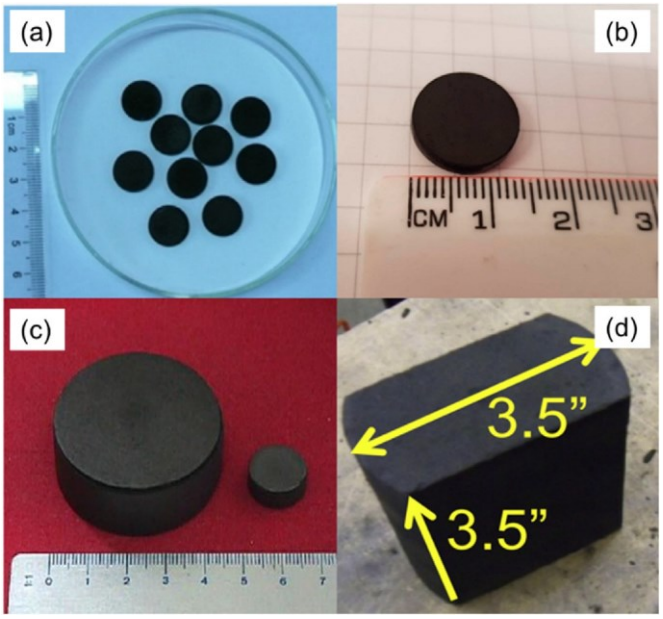

Fig. 1. Photographs of CM: nanomesh graphene binder-less monolith (a), Reprinted from Particuology, Copyright (2013), with permission from Elsevier [36] Activated carbon disc prepared from carbon sphere and mesophase pitch (b), Reprinted with permission from Ref. 63. Copyright 2019 American Chemical Society [69] ACM2, made of Spanish anthracite, with different dimensions (c), Reprinted from Microporous and Mesoporous Materials, Copyright (2008), with permission from Elsevier [24] Monoliths made from sawdust (d). Reprinted from Fuel, Copyright (2017), with permission from Elsevier [55].

2.2. Biomaterials for carbon monolith synthesis

Various biomaterials can be used to prepare activated carbons and CM, and each carbon precursor has its unique advantages. Many starting materials are low–cost and naturally abundant, such as anthracite, sucrose, rubber, sugarcane molasses, and even human hair [25,29–31]. Human hair has been used to fabricate CMs with potassium hydroxide (KOH) as an activation agent, and the resultant carbons showed a high surface area and relatively good microporosity, using the Brunauer–Emmett–Teller (BET) surface area theory. Scanning electron microscope (SEM) imaging and transmission electron microscope (TEM) imaging confirmed the microporous nature of these hair–based CMs (Fig. 2) [31]. A CM from Mongolian anthracite–based (MRA) activated carbon was synthesized with carboxymethyl cellulose as a binder [25]. The adsorption results indicated that the gravimetric methane capacities of the CM increased with an increased surface area. MRA was used as a carbon source for this study due to its low ash content, absence of carbonization, high bulk density, and its physical strength. Due to its intrinsic strength and density, MRA is ideally suited for high pressure adsorption processes, especially for ANG applications [25].

Polymer precursors synthesized from hydroquinone, urotropine, and furfural have been synthesized using poly vinyl alcohol (PVA) as a binder to create the monolith. The use of these small organic molecules in powder form allowed for the creation of aromatic compounds that are parallel stacked, avoiding empty domains that are counter to adsorption of methane [32]. However, the adsorption kinetics have shown that monoliths have a slower diffusion rate than powder counterparts [33]. The slow diffusion rates can be alleviated using carbon nanofibers as the precursor material due to the clusters retaining their shape and larger surface area even after pyrolysis [34,35].

Carbon materials like graphene can also be used for carbon monolith preparation. For instance, Ning and co-workers selected nanomesh graphene as a carbon source with porous MgO layers as the template. Nanomesh graphene was formed by methane crackling which is done by having the MgO layer template fed through heated methane flow, resulting in nanomesh graphene. Three types of graphene powders were produced with different rinsing agents. The powders were pressed into monolithic shapes directly under a specific pressure with no further heating (Table 1). The methane adsorption of the CM was 236 V/V at 9 MPa. Graphene is a good candidate for monoliths due to its ability to be formed into monoliths without the need for a binder. This binderless formation was achieved due to graphene's unique structure and ability to be stacked while maintaining its high surface area and bulk density [36]. Graphene can also be mixed with other carbonaceous materials, such as lignin, and put through a series of heating synthesis, including hydrothermal and pyrolysis, for the final CM [37]. The largest group of precursors are lignocellulose biomaterials, as the specific structure of cellulose benefits the production of high microporosity [13,38]. The lignocellulose materials widely used for CM preparations

include corn grain, olive stone, coffee husk, rice husk, banana peel, and peach pit, amongst others [39–44]. For instance, Molina–Sabio and co-workers selected olive stones as a starting material, with a particle size in a range of 0.1–0.5 mm [45]. Beech wood has been used to create monoliths with a porous surface with micropores measuring 1 nm in diameter [46]. Lignocellulose biomaterials materials show many advantages, such as low cost, widely available biosourced precursors, and high chemical stability with limited toxicity [47]. Also, these carbon rich materials through tailoring, have surface areas greater than 3500 $m^2\ g^{-1}$ and have the development of micropores with a volume less than 1 $cm^3\ g^{-1}$ [48]. These materials are also suitable for binder free methods that researchers utilize to avoid pore blockage [22].

2.3. The role of binder

The binders play an essential role in combining activated biocarbon powder into a CM. Some examples of binders frequently used are humic acid–derived sodium salt (HAS), PVA, Novolac PR binder from Water Sutcliffe Carbons (WSC), Teflon (TF), and adhesive cellulose-based binder (ADH). These binders ensure that the monolith will stay as one solid structure and not crumble during application. However, WSC and ADH have the highest adsorption, 95% and 94% of V_{N_2}, and 105% and 91% of V_{co_2} respectively, compared to theoretical values from previous tests [27]. In contrast, PVA had the lowest at 18% of V_{N_2} and 39% of V_{co_2} regarding theoretical values. The high density created by the binder was also an essential factor as it correlates to high methane volumetric uptake [27].

Among these CMs, the ones prepared with PVA as a binder were found to have a high density of 1.00 g cm^{-3} but exhibited the least nitrogen gas adsorption due to a low microporosity. The next highest density was the CM with WSC as a binder, which had a density of 0.58 g cm^{-3}. For methane adsorption, CMs with WSC, ADH, and TF as a binder showed the highest methane adsorption capacity of 126 V/V, 120 V/V, and 114 V/V at 298 K and up to 4 MPa, respectively. Due to the highest N_2, CO_2, and methane adsorption along with good density, WSC was discovered as the best binder for CM preparation [27]. Once the optimal binder (WSC) was selected for the precursor, Spanish anthracite, the most effective concentration of binder needed to be determined. Lozano–Castelló and coworkers found that excess binder can lower the adsorption capacity, but less binder can affect structural integrity. By adjusting the amount of binder, resultant CMs with 10, 15, and 20 wt% of WSC binder were made and denoted WSC 10, WSC 15, and WSC 20, respectively. WSC 10 was found to be the minimum amount of binder for the formation of a monolith with a homologous structure. WSC 10 did show a slightly higher methane adsorption capacity than WSC 15 but with a lower density (0.53 g cm^{-3}).

However, WSC 20 had the lowest methane adsorption and had the same density as WSC 15, indicating it was not beneficial to add more binder after reaching 15% (Fig. 3). WSC 15 was found to contain the optimal amount of binder as it had the highest adsorption, 1.07 $cm^3\ g^{-1}$ V_{N_2}, and 0.63 $cm^3\ g^{-1}$ V_{co_2}, with the highest density of 0.58 g cm^{-3} (Table 1) [27]. The use of polymers was used to create nanoporous carbon materials for methane storage. The materials can be formed into monoliths with the use of PVA.

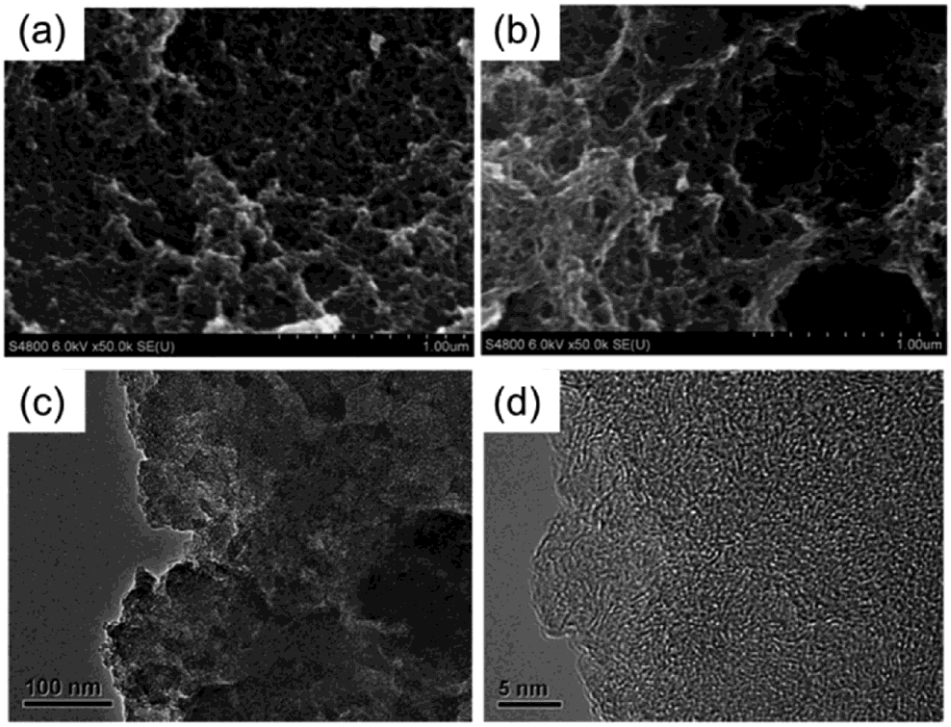

Fig. 2. The SEM (a and b) and TEM (c and d) images of the activated carbon monolith obtained from human hair. Republished with permission of Royal Society of Chemistry (2011), permission conveyed through Copyright Clearance Center, Inc [31].

Table 1
Comparison of monoliths from different precursors.

Form (Ref. #)	Precursor	Activation Agent	Binder (wt%)	Adsorbate	BET surface area	Volumetric uptake	Gravimetric uptake
Monolith [1]	Phenol-based activated carbons	H_2O	Poly vinyl alcohol (PVA) and polyvinyl pyrrolidone (PVP) binders 5 wt%	Methane	2200 m^2 g^{-1}	48 V/V	9.76 mmol g^{-1}
Monolith [14]	Isotropic pitch-derived carbon fibers	CO_2	powdered phenolic resin	Methane	2451 m^2 g^{-1}	159 V/V	e
Monolith [25]	Mongolian raw anthracite	KOH	carboxy-methylcellulose (CMC) sodium salt	Methane	1460 m^2 g^{-1} (Volumetric) 2299 m^2 g^{-1} (Gravimetric)	162.2 V/V	12.5 mmol g^{-1}
Monolith [27]	Spanish anthracite	KOH	Proprietary binder from Waterlink Sutcliffe Carbons 15 wt%	Methane	e	126 V/V	e
Monolith [36]	Nanomesh graphene	e	Binder less	Methane	1451 m^2 g^{-1}	236 V/V	e

Compared to its powdered counterpart and other commercially available carbon adsorbents, these polymer–based materials exhibited higher bulk specific capacity 198/336 (Vt) cm^3 cm^{-3} [32].

Binders are often necessary to form carbon monoliths, but their addition can block pores, decreasing microporosity. Powdered activated carbon, for example, was converted into monoliths using silica sol, a colloidal solution of SiO_2 as a binder. The use of 3.0 mL of silica sol gel, when added to 2.4 g of the activated carbon gave the strongest monolith with a strength of 1.7 MPa, as compared to other monoliths in this experiment that did not use silica sol gel as a binder [49].

Different starting biomaterials may have a specific binder that works better than other binders to produce a high-quality carbon adsorbent. Balathanigaimani and co-workers investigated novel corn grain-based activated biocarbon and examined the binders PVA, polyvinyl pyrrolidone (PVP), and carboxymethylcellulose sodium salt (CMC) for the creation of CMs. The binders were added with different quantities and combinations to determine which binder worked best with the corn grain for CM production. After the best binder for the starting material was found, a comparison of methane adsorption was tested under different temperatures of 293.150, 303.150, and 313.150 K at 35 atm. Five CMs were initially created with MR–1/4, CMC at 5 wt% and 10 wt%, PVA at 10 wt%, PVP at 10 wt%, and PVA and PVP combination at 10 wt%. CMs were also created with MR–1/3 and MR–1/2, consisting of CMC at 5 wt% and PVA/PVP at 10 wt%. In a comparison of the above CMs, CM with CMC at 5 wt% had the high density of 0.292 g cm^{-3}. Methane adsorption tests were conducted on the CM with CMC at 5 wt%. CM from MR–1/4 with CMC at 5% had the highest gravimetric methane adsorption of 13.73 mmol g^{-1}, due to having a high surface area (2647 m^2 g^{-1}) and pore volume (0.955 cm^3 g^{-1}). Also, CM from MR–1/2 with CMC at 5% had the highest volumetric methane adsorption ability at 100 V/V due to having the highest density [39]. These results indicated that CMC at a ratio of 5 percent is the best binder for CM preparation from corn grain.

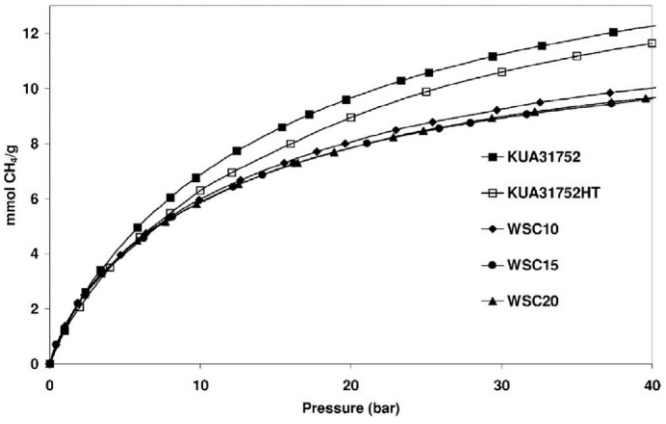

Fig. 3. Methane adsorption isotherms at 298 K corresponded to the powdered activated carbons, and the activated CMs prepared with different amounts of WSC binder. KUA31752 and KUA31752HT were the starting carbon powder and the carbon powder heat treated at 750 °C. Reprinted from Carbon, Copyright (2002), with permission from Elsevier [27].

However, excess binder can cause pore blocking in the final CM products. Muto and co-workers explored using cotton fibers coupled with carbon dioxide activation to counteract pore blocking caused by binders. Carbonized cotton fibers and phenol resin were combined, and the mixture was heated, pressurized, and baked for a desired time. The addition of a binder can significantly reduce the porosity of monoliths; therefore, the porosity was tailored by activation with carbon dioxide. By adjusting the resin ratio to the cotton mixture, the maximum adsorption capacity for the products was achieved. For comparison, products without activation and just two–hour activation were also synthesized. Two carbons were made with a ratio of 100 resin to 0 cotton mixture to determine the structure formed by pure resin. Then four products with 2 h of activation were obtained, each with different ratios of resin to cotton mixtures of 90:10, 85:15, 80:20, and 75:25 [50].

As the cotton ratio increased, methane adsorption, pore volume, and surface area increased. Still, between the ratio of 80:20 and 75:25, the increased amounts became much smaller,

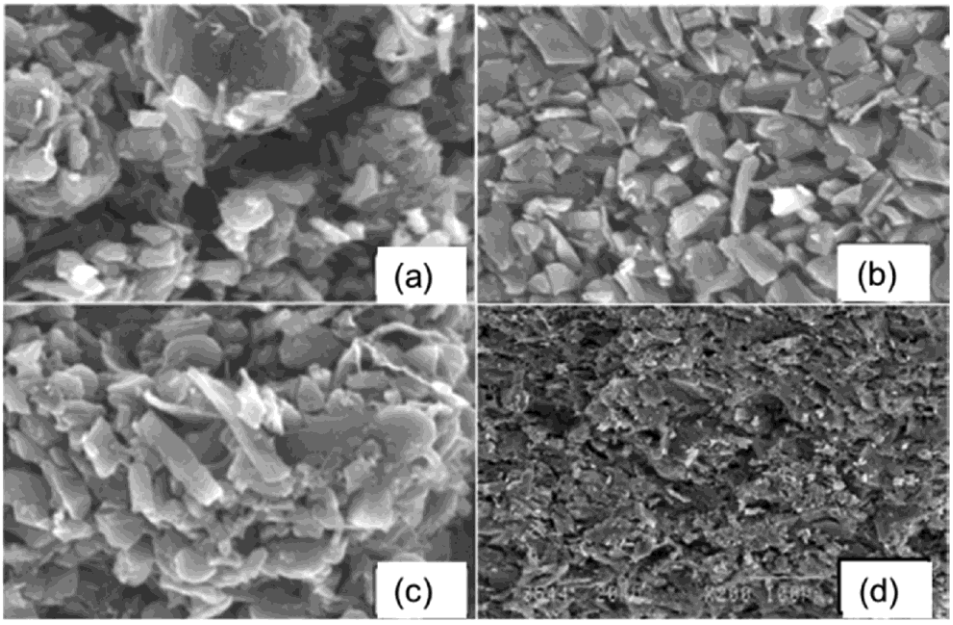

Fig. 4. SEM analysis of representative activated CMs: (a) 25% carbonized cotton fiber and phenol resin activated for 5 h, (b) 25% carbonized cotton fiber and phenol resin activated for 2 h, and carbonized cotton fiber. (c) Reprinted with permission from Ref. 50. Copyright 2005 American Chemical Society [50] SEM pictures of three activated CMs formed with WSC (d). Reprinted from Carbon, Copyright (2002), with permission from Elsevier [27].

indicating that increasing the ratio of cotton further is unnecessary. After the samples with 80:20 and 75:25 ratios were rerun for 5 h, a sufficient activation time was found. As activation time increased, there was not much difference in pore shrinkage, but there was a significant increase in adsorption capacity, surface area, and total pore volume. SEM showed structural comparisons and different morphologies between biocarbons with varying activation times (Fig. 4). The ratio of 75:25 had the highest cotton content of all the reactions, which led to an adsorption of 245 $cm^3\ g^{-1}$. The optimal activation time and the proper mixture combination shows the highest methane storage capacity of 143 V/V at 35 ºC and 3.5 MPa (Table 2) [50]. Machnikowski and co-workers' experiment also showed the binders impact Novolac, a commercial activated carbon. CMs with polyfurfuryl alcohol (PFA) exhibited the highest gravimetric methane uptake due to the high porosity of 0.69 $cm^3\ g^{-1}$ and surface area of 1517 $m^2\ g^{-1}$, as well as the highest volumetrically due to excellent density [51].

Machnikowski and co–workers noticed that porosity gets inhibited and blocked during the baking process for the monolith formation, allowing less methane to be absorbed. Carbon dioxide was used to activate the pores and to open those channels. The activated carbon in the experiment was semi–coke activated with KOH with a binder of PFA. CMs were created with different percentages of PFA, named as MA–PC–2 with PFA as 23 wt%, MA–PC–3 with PFA as 33.3 wt%, and MA–PC–4 with PFA as 28.6 wt%. The monoliths were activated with CO_2, and the highest micropore volume of 0.822 $cm^3\ g^{-1}$ was achieved. In contrast, the highest pore volume for the baked monoliths is only 0.472 $cm^3\ g^{-1}$ (Fig. 5) [52].

There are many binders that could be used with three most prolific being PVA, PVP, and phenol resin. These all worked well at maintaining a monolithic structure while also lessening the pore blockage that is common with the introduction of a binder to activated carbon. The key thing would be to reduce the amount of binder enough that a monolith is still able to be formed, but little more, as the excess binder is more likely just to block pores and lead to lower methane uptake.

2.4. Binder-less methods for carbon monolith preparation

CMs also can be fabricated by using a binder-less method. Binder-less formation of monoliths has beneficial advantages over the binder method. Firstly, binders often hinder pore

Table 2
Comparison of monolithic and powder products from different precursors.

Form (Ref. #)	Precursor	Activation Agent	Binder (wt%)	Adsorbate	BET surface area	Volumetric uptake	Gravimetric uptake
Monolith [13]	Olive stones	$ZnCl_2$ and CO_2	e	Methane	e	110 V/V	e
Monolith [50]	Carbonized cotton fiber	CO_2	Phenol resin	Methane	1440 $m^2\ g^{-1}$	143 V/V	e
Monolith [54]	Mesophase self-sintering carbon	KOH	Binder less	Nitrogen	2850 $m^2\ g^{-1}$	e	z41 mmol g^{-1}
Powder [31]	Human hair	KOH	N/A	Methane	2380 $m^2\ g^{-1}$	e	5.5 mmol g^{-1}

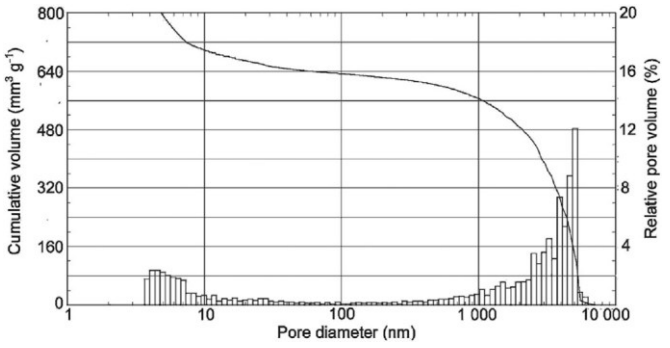

Fig. 5. Pore size distribution for the monolith MA–PC–3/PFA. Reprinted with permission from Ref. 52. Copyright 2010 American Chemical Society [52].

development and block pores in the final biocarbon products, resulting in a lower methane uptake [50]. Secondly, the addition of a binder will increase the density of an activated biocarbon and make a more solid structure in the form of a monolith. However, the monolith preparation without a binder can achieve a more uniform structure that helps improve the methane storage capacity. Finally, the binder-less method is greener as fewer chemicals are needed and has lower overall costs. It should be noted that a high-density CM also can be synthesized without a binder but under high pressures in a mold.

For instance, Romero–Anaya and co-workers reported one binder-less method for CM preparation from sucrose–derived spherical carbon. The spherical biocarbon was first carbonized using a hydrothermal apparatus at 200 °C. Then, the product was placed into a mold, where pressure and heat were applied to form a monolith. Further activation was conducted using carbon dioxide at 1153 K with different activation times (0, 10, 15, and 18 h). The monolith with 18-h activation exhibited a high porosity of 1.38 $cm^3\ g^{-1}$ and surface area of 3800 $m^2\ g^{-1}$, which is the best candidate for methane storage. It demonstrated the highest storage capacity for methane of 278 g L^{-1} at room temperature and pressures up to 20 MPa. The SEM showed that the carbon did create a cohesive monolith (Fig. 6), indicating that it is still possible without using a binder while exhibiting high methane adsorption [22].

In comparison, Guan and co-workers used ammonium–form zeolite Y as a template, which was combined with PFA as a carbon source. This mixture was then pyrolyzed. When removing the template from the carbon, an acid wash was performed. Monoliths were then formed by compacting the resulting carbon powder under a heated press, reaching 200 °C for 4 h. The structural features of the carbon powder and final carbon monolith was confirmed by using SEM. The carbon powder showed many voids, which disappear once the powder is packed into a monolith form. At the same time, the monolith showed more apparent distinctions of layering or turbostratic structures, indicating the possible formation of graphite [53]. The methane adsorption capacity test showed that the monolith form had improved adsorption of 127 V/V compared to the powder (60 V/V) (Fig. 7a). In addition, there was an increase of three-fold in the bulk density. The mechanical strength of the monolith was also examined and showed excellent mechanical strength and resilience [53]. Both above reports

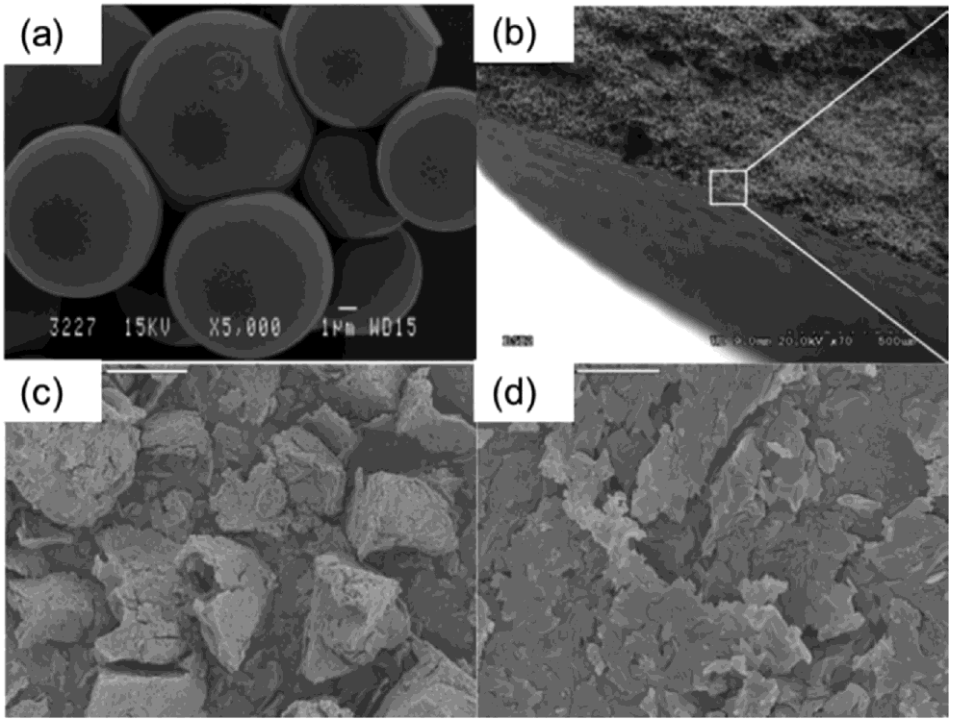

Fig. 6. SEM images of spherical biocarbon (a) and activated carbon monolith (b). Reprinted from Microporous and Mesoporous Materials, Copyright (2019), with permission from Elsevier [22]. SEM images of powdered activated carbon (c and d). Reprinted with permission from Ref. 51. Copyright 2012 American Chemical Society [51].

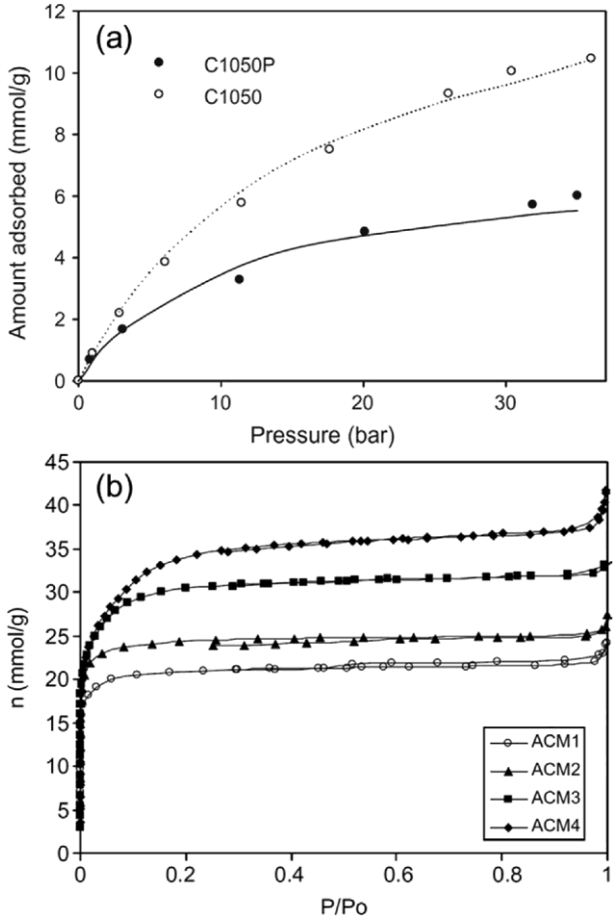

Fig. 7. Methane isotherm at 25 ºC (symbols) and the optimal fittings of Langmuir equation (lines) for ammonium–form zeolite Y carbon (a). Reprinted from Energy Conversion and Management, Copyright (2011), with permission from Elsevier [53]. N_2 adsorption isotherms at 77 K for sucrose derived spherical carbon-based CMs, ACM x where x represents the ration of KOH/carbon (b). Reprinted from Carbon, Copyright (2008), with permission from Elsevier [54].

showed that effective carbon monolith fabrication methods with a strong mechanical strength are comparable to monoliths created with a binder.

Finally, a binder-less CM formation method with mesophase–based mediums was explored by Ramos–Fern'andez and co-workers. The starting material is mesophase self–sintering carbon (MSC), derived from mesophase pitch (MP). Firstly, the MP was pyrolyzed and soaked in KOH for two or 4 h. The solid that resulted from this process was mesophase self–sintering carbon, produced when the MPs were at their boiling point. The MP and the MSC were activated with KOH for 30 min. Then, the activated carbons were pressed into monoliths under various pressures, ranging from 100 to 400 MPa. The monoliths were further heat treated and washed with HCl acid. Finally, the monolith was baked dry for 24 h before gas adsorption/storage tests. The MSC showed a higher softening point and viscosity when compared to MP, making it more fragile. The MSC had low volatility and had the top carbon and mesophase content. MSC is a rigid monolith and breaks apart back to a powder after handling. The change in applied pressure did not significantly affect the various monoliths made from MSC [54]. The MP monoliths broke apart effortlessly under the pressure of 100–220 MPa and did not survive the formation process. However, under 400 MPa pressure, a rigid monolith was created to survive the manipulation. For determining the best amount of KOH for activation, monoliths were created from MP with 4 h of soaking and pressed at 400 MPa. The monolith with the ratio of 4:1 of KOH to carbon had a micropore volume of 0.95 P/P_0 (Table 2), showing the best route to form a highly microporous CM [54]. While the binder-less method may lessen pore blocking, not all starting materials are conducive to form into a monolithic product without a binder.

2.5. The role of activation temperature

The activation temperature also plays a vital role in pore generation and adjustment of the pore size. For example, Djeridi and co-workers studied the effect of activation temperature on porosity development. Olive stones were used as a starting material, and CMs were fabricated with a binder-less method. The olive stones were chemically activated by H_3PO_4, and the resultant biocarbon powder was compressed into a monolith. Then, the monolith was further activated under a nitrogen flow for 3 h with the desired activation temperature (350 ºC–1000 ºC). The porosity measurements indicate that the surface area and microporosity decrease as the activation temperatures increase. However, this trend does not hold for monoliths ACP410 activated at 410 ºC and ACP1000 activated at 1000 ºC. These have a higher surface area and microporosity than the ACP350 activated at 350 ºC. ACP410 has the highest methane adsorption, surface area, and better porosity than ACP1000. These results show that as the activation temperature increased, the micropore size distribution widened (Fig. 8) [40].

3. Activation agents of CM preparations

Activation of the monoliths is performed to increase adsorption capacity, as more micropores can be developed and

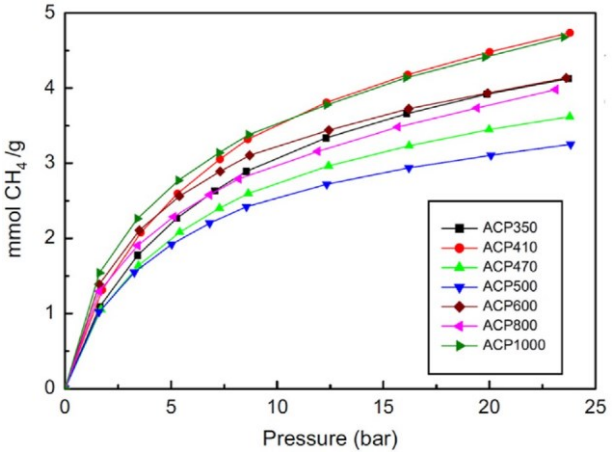

Fig. 8. CH_4 adsorption isotherms at room temperature for a binder-less olive stone monolith. The CMs were named as ACP*x*, here *x* means the activation temperature in ºC. Reprinted from Materials Letters, Copyright (2013), with permission from Elsevier [40].

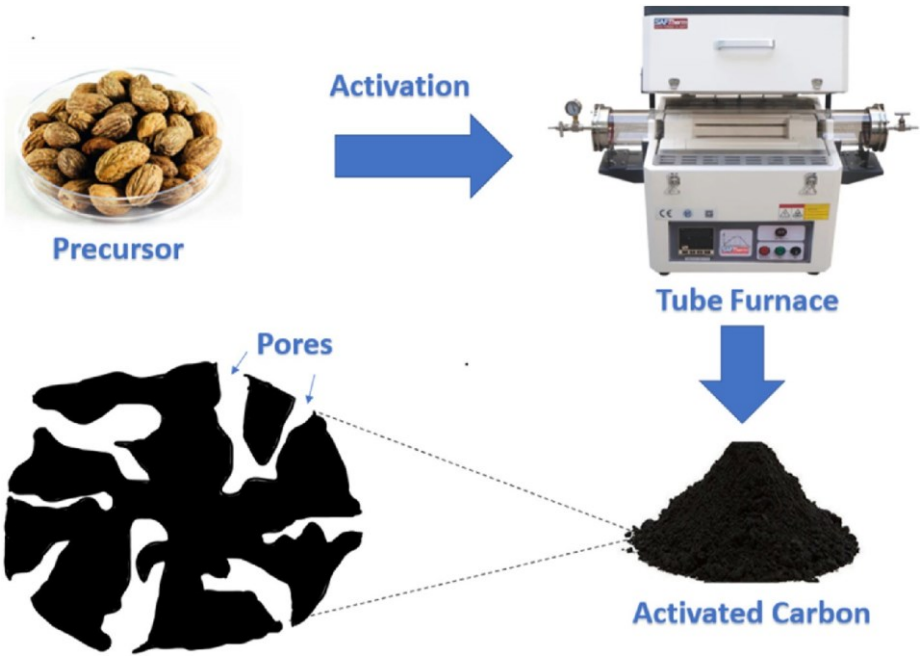

Scheme 2. Activated carbon processes from biomass precursor.

expanded during the activation process, leading to higher surface area and making them more optimal for methane adsorption. Secondary activation with monoliths can tailor the pore size further and unblock pores blocked by a binder. There are two main types of activation that can be performed for CM modification. The first is chemical activation with KOH, $CaCl_2$, $ZnCl_2$, or H_3PO_4. These chemicals are assessed and used with different amounts to determine the optimal amount of activation to improve the methane uptake. The second activation methods are the physical ways by flowing steam or CO_2, typically performed by placing the sample in a tube furnace and then flowing the activation agent. Scheme 2 shows a general process of activation to make high porous carbons. Both chemical and physical activation methods can be used in monolith preparation, and it has been demonstrated that the combination of these two methods can increase the pore volume and pore size in CMs (Table 3).

3.1. Chemical activation with KOH

Byamba–Ochir and co-workers studied Mongolian raw anthracite (MRA) with KOH as an activation agent for CM preparation. The monoliths are made from different ratios of MRA to KOH ranging from 1:0.5 to 1:4, annotating the ratio in the monolith name. The binder used was CMC, and the binder contents were either 3, 5, or 10 wt%. The monoliths were compressed at four different pressures, 10, 25, 45, and 65 MPa. As the concentration of KOH increased, there was a decrease in packing density, but an increase in surface area and pore volume due to more KOH generated pores. While examining volumetric adsorption of monolith PMAC1/2–3–65, where ½ is the activation agent ratio, 3 is the percent of binder, and 65 is the pressure used in MPa, the highest adsorption of 162 V/V under a pressure of 3.5 MPa and a temperature of 293 K was observed. As expected, the increase in binder concentration caused a decrease in volumetric adsorption capacity. However, the KOH ratio was most influential on the gravimetric adsorption amount, as increasing KOH decreased the density of the final products. Still, this study found an optimized proportion of carbon to KOH at 1:2 [3].

Rash and co-workers studied making a CM from sawdust with KOH as an activation agent. The starting material was activated twice, once with a commercial product and then further activated with a ratio of 2:1 with KOH to obtain biocarbon. Polyvinylidene chloride–co–vinyl chloride was used as a binder, and the mixture was compressed under pressure and heat to create a large monolithic structure. For the final CM product, the surface area went up to 2800 $m^2\ g^{-1}$ and had a pore volume of 2.08 $cm^3\ g^{-1}$, with a much narrower pore

Table 3
Comparison of monolith, powder, and granular powder from different precursors.

Form (Ref. #)	Precursor	Activation Agent	Binder (wt%)	Adsorbate	BET surface area	Volumetric uptake	Gravimetric uptake
Granular [72]	Olive pulp, peel, and seed	$ZnCl_2$	N/A	Methane	913 $m^2\ g^{-1}$	59 V/V	e
Granular [73]	Commercial	e	N/A	Methane	1426 $m^2\ g^{-1}$	z120 V/V	z8 mmol g^{-1}
Monolith [74]	Victorian brown coal	CO_2	e	Hydrogen	973 $m^2\ g^{-1}$	e	1.2823 mmol g^{-1}
Powder [44]	Peach pits	H_3PO_4	N/A	Methane	1560 $m^2\ g^{-1}$	e	z0.16 g g^{-1}

size distribution than its precursor, the activated biocarbon powder. However, the monolith possessed less porosity due to the binder clogging the pores, resulting in a smaller methane volumetric adsorption capacity. For the adsorption measurement, the CM was placed into a 40 L flat panel tank filled with methane at a pressure of 3.5 MPa. At 3.5 MPa, the volumetric adsorption capacity was 105 V/V, showing the CM has a 94 percent capacity of the internal tank volume. While increasing the pressure to 4.3 MPa, the volumetric storage capacity correspondingly increased to 172 V/V [55]. In these studies, KOH was an effective activation agent, as more micropores were being developed. Interestingly, based on these studies, a ratio of 1:2 for carbon to KOH was discovered to be the most effective for maintaining density and good porosity. However, this may not always be true for all precursor biomaterials such as corn cobs. As a result, the optimized ratio was 1:1 for the highest methane adsorption capacity [56].

3.2. Chemical activation with $CaCl_2$

$CaCl_2$ is also an effective carbon activation agent. For example, Vargas and co-workers investigated using $CaCl_2$ for biocarbon activation for CM preparation from African palm shells. For comparison, the raw material was also activated using H_3PO_4 and $ZnCl_2$. Various chemical concentrations were tested to find the optimal ratio for each activation agent. The resultant powder carbons were made into monoliths without a binder and instead used an impregnation and compression method. The monoliths were shaped with honeycomb channels. Granular activated carbon activated with H_3PO_4 at 48% and CM activated with $CaCl_2$ at 2% had the highest micropore volume of all the samples. While the CM product with $ZnCl_2$ at 48% had ultra–microporosity, it was hampered because it had a small surface area. However, the CM activated with $CaCl_2$ at 2% exhibited the highest methane adsorption capacity at 298 K and 4500 kPa, indicating $CaCl_2$ is an effective agent for African palm shells (Fig. 9).

The adsorption for the $CaCl_2$ activated monolith at 2% is comparable to other $CaCl_2$ activated carbon at 3% [57]. It is worth pointing out that, unlike most activation agents, $CaCl_2$ at a higher percentage is not beneficial for increased methane adsorption.

3.3. Chemical activation with H_3PO_4

Another activation agent that has been widely used for improving the CM gas adsorption is H_3PO_4. For instance, Molina–Sabio and co-workers selected H_3PO_4 to make CM with olive stone as a starting biomaterial. No binder was used; instead, the impregnation technique was used to create a binder-less monolith. The CMs were made from different concentrations of H_3PO_4, at 0.21, 0.28, 0.35, and 0.42. Then, the CMs were further activated with carbon dioxide to create various burn-offs, the percentage of the initial amount burned off ranging from 10 to 40%. The bulk density decreased as the H_3PO_4 ratios increased, leading to a higher porosity in the CMs. The microporosity of the monoliths shows a substantial increase as the H_3PO_4 concentration increases, but after reaching 0.35, the micropores start to transform into mesopores. CM with H_3PO_4 being 0.42 showed the highest microporosity. However, methane adsorption tests showed that CM made with H_3PO_4 being 0.35 exhibited the highest adsorption capacity compared to the monolith at 0.42. For CMs made with a concentration of 0.35 H_3PO_4 methane adsorption increased as burn off increased, with the CM made from H_3PO_4 at 40% burn-off had methane adsorption of 150 V/V under a pressure of 3.4 MPa and 25 °C [45].

MacDonald and co-workers also chose H_3PO_4 as the activation agent and examined the ratio for producing CMs. Peach pits were selected as the starting biomaterial. However, the resultant activated biocarbons failed to transform into a CM but instead came out as an extrudate. The FOS 6 series was done at a 2 mL of H_3PO_4 ratio to every gram of peach pit. The highest surface area achieved was 1560 $m^2\ g^{-1}$ for the sample prepared at a temperature of 500 °C. Despite having a lower surface area, the carbon obtained at 600 °C exhibited higher methane adsorption at 298 K to 3.5 MPa. These results indicated that macropores and mesopores are not beneficial for methane adsorption [44]. Also, the activation agent that works well with the starting biomaterial is critical for carbon preparation and improved methane adsorption.

3.4. Chemical activation with $ZnCl_2$

Almansa and co-workers used $ZnCl_2$ to activate olive stone and used the resulting activated biocarbons for CM preparation. Five experiments were conducted separately, with mass percentages of $ZnCl_2$ being 19, 24, 32, 38, or 48 wt%. Then, the carbon was pressed into a mold at 130 MPa, at 150 or 300 °C. Afterward, two discs were placed under a carbon dioxide flow for further activation. As the $ZnCl_2$ content

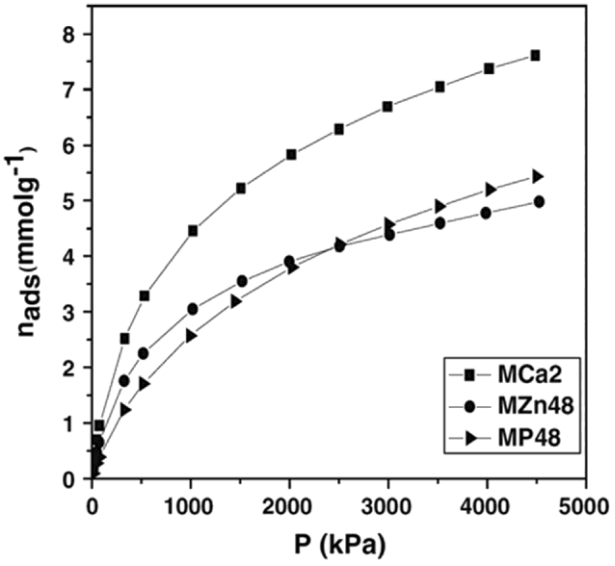

Fig. 9. Adsorption isotherms of CH_4 at 298 K for CMs made from African palm shells. These CMs were activated with $CaCl_2$, $ZnCl_2$, and H_3PO_4, separately. Reprinted by permission from Springer Nature, Copyright (2013) [57].

increased, a trend showed that more nitrogen was adsorbed under the same temperature and pressure. The CMs made from $ZnCl_2$ concentration range of 32–38 wt% showed the highest methane uptake gravimetrically and volumetrically. The compression temperature also played an essential role in affecting the methane adsorption, as monolith discs obtained at 150 °C had a better methane adsorption capacity of 96 V/V than the one obtained at 300 °C (79 V/V).

The discs were further impregnated with 0.2 g g^{-1} $ZnCl_2$ and activated again under a carbon dioxide flow to improve the methane adsorption. The discs activated at 150 °C showed a decrease in interparticle space, while the discs activated at 300 °C had increased interparticle space, which was found by looking at the distribution of the volume of the carbon skeleton, micropores, and non-micropores. As expected, there was an increase in methane adsorbed for biocarbon discs activated at 150 °C with an improved methane adsorption capacity at 110 V/V at 25 °C and 3.4 MPa pressure (Table 2) [19].

3.5. Physical activation with steam

Physical activation is an alternative to chemical activation as it can be low cost and more widely available. The carbon's physical activation can be conducted by both steam and carbon dioxide. Nitrogen flows have also been used as an activation agent, primarily for a secondary activation step [58]. While steam is widely used as an initial activation agent, steam is frequently used in conjunction with chemical activation to develop added porosity.

Additionally, the combination of chemical and physical activation methods is an excellent technique to control and generate microporosity. The chemical activation creates the pores, but the physical activation enlarges the pores [59]. Giraldo and Moreno–Piraj'an compared the nitrogen and steam activation with chemical activation, and the results indicated that steam activation has higher methane adsorption due to high surface area and pore volume [60]. Another example also found that biocarbons from rice husks exhibited improved methane adsorption based on physical activation with steam for 20 min at 900 °C [42].

3.6. Physical activation with CO_2

Carbon dioxide is another agent of physical activation for pore generation inside biocarbons and is quite beneficial in increasing methane adsorption. For example, Marco–Lozar and co-workers examined what factor has the greatest effect on methane adsorption and selected carbon dioxide as an activation agent to improve the porosity. Activated carbons with high density were commercially purchased from BrightBlack, labeled A1 and A3. The carbons were pyrolyzed under a nitrogen flow with different activation times, with A1 being activated the longest. Monolith A3 was further activated with carbon dioxide at various activation times of 12, 24, 36, and 48 h. Two monoliths were made. One was M3M, which used highly activated carbon preparation and a polymeric binder. Another one, K1M, was made from Spanish anthracite that was chemically activated with KOH, then the polymeric binder was added with 15 wt% for monolith synthesis. With the A3 series of monoliths, it was shown that as activation time increased, the adsorption capacity, surface area, and micropore volume also correspondingly increased, but as expected, the density decreased. For methane adsorption, pore size is a crucial factor. K1M and M3M had a high microporosity, while the A-series had a narrow pore size distribution. The gravimetric results showed that A3 with 48-h CO_2 activation, closely followed by M3M, had the highest amount of methane adsorbed at 3.0 MPa and 150 °C (Fig. 10). For volumetric adsorption, the A3 series was the top, and A3 with 48-h activation was the best carbon adsorbent as it had the highest methane adsorption and microporosity [61].

Prauchner and co-workers also improved methane adsorption by using extra physical activation to increase the pore

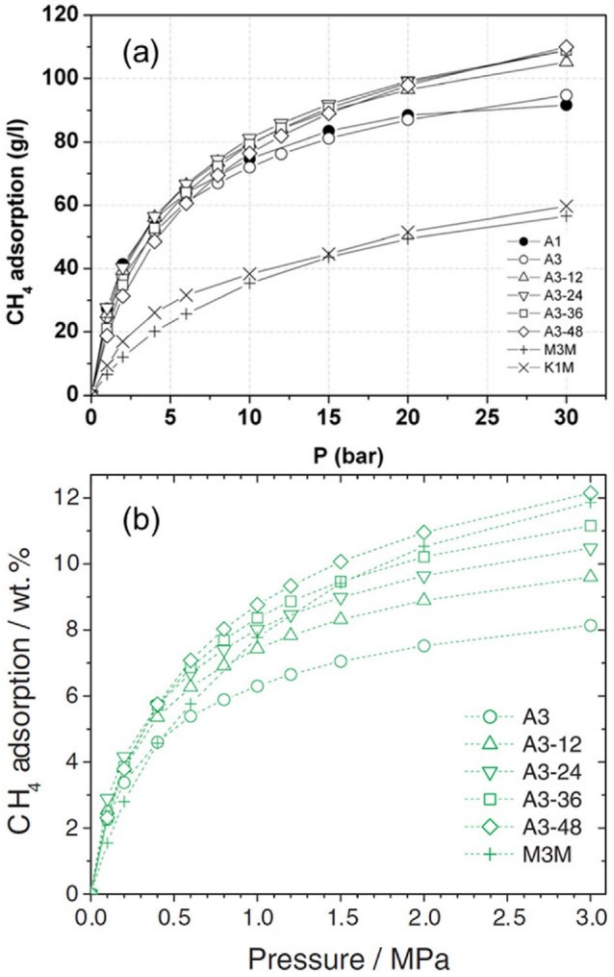

Fig. 10. CH_4 excess adsorption isotherms at 25 °C on a volumetric basis for A3 with no CO_2 activation, A3-x here x means the CO_2 activation time of the powder, M3M Maxsorb monolith, and K1M lab made monolith (a). Republished with permission of Royal Society of Chemistry 2008; permission conveyed through Copyright Clearance Center, Inc [61]. Isotherms from CH_4 adsorption at room temperature on a gravimetric basis for A3 with no CO_2 activation, A3-x here x means the CO_2 activation time of the powder, and M3M Maxsorb monolith (b). Reprinted with permission from Ref. 63. Copyright 2015 John Wiley and Sons [63].

size. The carbons were made from coconut shell endocarps as the raw ingredient, and four different activated biocarbons were obtained, including two based on chemical activation using H_3PO_4 or $ZnCl_2$. The other two products were raw carbon after chemical activation by H_3PO_4 or $ZnCl_2$, followed by physical activation with CO_2. Then, CMs were prepared with different activated biocarbons through a binder-less method. The chemical activation method with H_3PO_4 and $ZnCl_2$ showed a higher surface area and an increased micropore volume than the physical activation method. However, CMs with CO_2 activation had higher methane adsorption due to narrow pore distribution. Therefore, the combined chemical and physical activation yielded the best results and were chosen for improving methane adsorption. These results indicate it is better to do a softer chemical activation, despite macropores still being present, and in turn, more intense gasification with the CO_2 to achieve the best porosity. CM made from this combined physical and chemical activation using H_3PO_4 exhibited volumetric methane adsorption of 145 V/V at 3.5 MPa pressure and 25 ºC [62]. However, CM created from this combined activation but using the $ZnCl_2$ instead of H_3PO_4 had low methane adsorption due to the structural collapse [62]. CO_2 was also used to activate commercial CMs, and they exhibited an improvement in methane adsorption. For example, Kunowsky and co-workers found that carbon dioxide activation for 48 h on commercial CM (BrightBlack) increased methane adsorption by 5.5 times (Fig. 10) [63].

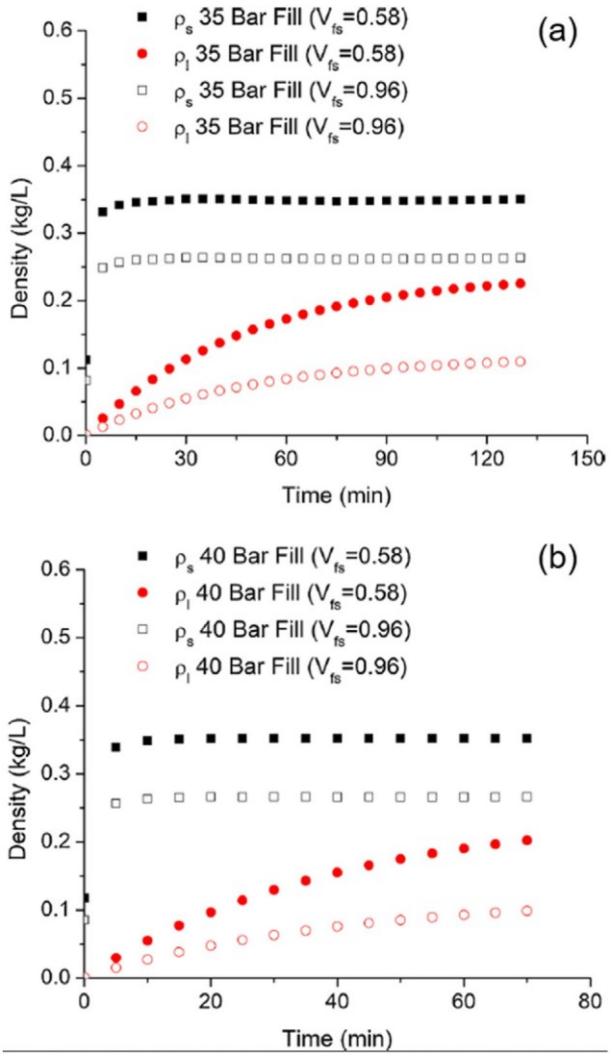

Fig. 11. Evolution of micropores (r_s) and mesopores (r_l) with time for the 35-bar inlet methane fill (a). Evolution of r_s and r_l with time for the 40-bar inlet methane fill (b). Reprinted from Journal of Energy Storage, Copyright (2018), with permission from Elsevier [3].

As mentioned above, this combined activation method greatly benefits methane adsorption because chemical activation limits the number of macropores formed, and the physical activation creates micropores. Also, biocarbon products made with this combined methodology show a narrower pore size distribution than carbons prepared just from physical activation.

The amount of activation agent is also a key factor to adjust in the activation process as too little agent cannot form enough pores, while too much activation agent will cause pores that are too large to capture and store methane. Chemical and physical activation both have their advantages and disadvantages. However, by using both chemical and physical activation, the CMs normally showed a better pore development than just using a single activation method.

4. Characterization of porosity for CMs

The surface area and pore size of CMs are the most critical factors affecting adsorption capacity. Regularly, the porosity parameters of CMs are characterized by using nitrogen, CO_2, and Kr adsorption. Sometimes, other gases, such as hydrogen and butane, are used for adsorption tests to determine the pore size distribution since these gases have different size diameters, and they can show a clearer picture of pore size distribution. In addition to the gas adsorption tests, computational simulations based on non–local density functional theory can be used to confirm or predict the porosity and, most notably, the microporosity inside the monolith. However, CMs with narrow micropores can have lower nitrogen adsorption, as nitrogen isotherms cannot accurately predict the adsorption of narrow micropores [64]. Grand Canonical Monte Carlo (GCMC) simulations of the isotherms can be used to understand the methane adsorption behaviors. However, it cannot yet anticipate how the gas will interact with the activated carbon as it does not consider surface chemistry and gas adsorption equilibrium [65]. As shown in Fig. 11, the micropores will adsorb and have higher gas density, which means they fill up with the adsorbate first in a monolith, and, once the micropores are full, the mesopores will start to fill, and density will increase. The mesopores will only start to hold and adsorb the gas once the micropores have become fully saturated [3]. SEM can be used to visualize the void size and distribution of the microstructure for the CMs. Cao and co-workers looked at the optimal pore size and found that for volumetric and gravimetric uptake, the data showed that channels with a

diameter of 2.03 nm were optimal for increased methane uptake [66].

Computational simulations also can be used to understand the pore structures and symmetries inside the CMs. For instance, Kwiatkowski and Delgadillo used computational simulations to analyze the role of different activation agents for their effects on porosity generation. The computational analysis performed was the numerical clustering-based adsorption analysis (LBET) method derived from the uniBET method [67]. Data was taken from previously completed studies on biocarbon materials derived from African palm shells. The monoliths were separately chemically activated using $CaCl_2$, $ZnCl_2$, and H_3PO_4. Then, the nitrogen, carbon dioxide, and methane adsorptions were performed. The LBET analysis was conducted based on the data from these three kinds of isotherms. The results showed that the $CaCl_2$ activated monolith had limited pores with a low LBET score and a small nitrogen particle pore growth. However, the initial adsorption layer possessed high energy, indicating it was decently microporous but substantially mesoporous.

The data from the LBET is consistent with the BET and the Dubinin–Raduchkevich results, indicating it can match the current methods employed. The H_3PO_4 activated monolith results showed that the surface of the CM was homogeneous and had clusters of larger nitrogen particles than the previous monolith [67]. However, the monolith activated with $ZnCl_2$ was found to be heterogeneous. The adsorption volume of the first layer was close to half that of the other monoliths due to unfavorable energy conditions. These conditions led to poor adsorbate particle development, which suggested less methane adsorption. These results from the methane adsorption isotherm showed that the surfaces were highly heterogeneous. Based on these analysis data, $CaCl_2$ activated monoliths and H_3PO_4 activated monoliths showed branched methane clusters, while the $ZnCl_2$ activated monolith had smaller methane clusters. It also confirmed that lower energy for first layer gas molecule adsorption is beneficial for adsorption. On top of the first layer, the second layer on three products possessed typically tiny energy levels. Both $CaCl_2$ and $ZnCl_2$ activated monoliths have limited methane adsorption as they do not have a significant amount of micropores. The H_3PO_4 activated monolith had competitive adsorption as other clusters would impede adsorption. Based on these results, the LBET analysis can effectively determine the porosity and provide a more detailed analysis of carbon dioxide and methane adsorption isotherms [67]. Additionally, computational simulation data can supply information for further CM syntheses and structure predictions.

Porosity is the most important factor for methane adsorption. While both surface area and density lead to higher methane uptake, either factor is null if there are not pores for the methane to be stored in. With the knowledge of the optimal pore size and diameter, one can forecast how much activation needs to be done and if the methane adsorption will be sufficient.

5. Methane adsorption tests

Methane adsorption capacity increases under higher pressure, and methane adsorption is more effective for storage than compressed methane under higher pressures. Himeno and coworkers investigated various microporous CMs under high pressures for methane adsorption, including commercial Norit R1 Extra with peat, BPL with coal, Maxsorb with chalk, and A10 fiber with petroleum pitch, as well as one noncommercial activated carbon derived from coconut shells, labeled as ACA. The methane adsorption isotherms pressure reached 6000 kPa. Maxsorb showed the highest adsorption capacity of 15 N mol^{-1} kg^{-1} due to its highest surface area and porosity, followed by ACA, Norit R1 Extra, and A10 (Table 4) [68]. In many reports, the lab-made activated biocarbons were often compared with top commercial activated carbons such as Maxsorb for methane adsorption [12].

Also, Giraldo and Moreno–Piraj'an measured the adsorption capacity for biocarbons made from coffee husks under high pressure of 35 atm. The coffee husks were chemically activated using $ZnCl_2$ or KOH. Then, the resultant activated biocarbon was further fabricated into a monolith with PVA as a binder and shaped in a disc or a honeycomb.

The methane adsorption isotherms were performed up to pressures of 35 atm. The honeycomb shaped monoliths activated with $ZnCl_2$ had the highest surface area of 1326 m^2 g^{-1} and a pore volume of 0.86 cm^3 g^{-1}. The methane adsorption capacity was 130 V/V at 30 atm (Fig. 12). The plausible reason is that the honeycomb structure allows a faster diffusion of methane molecules than in the disc monoliths. For adsorbed methane, the $ZnCl_2$ activated honeycomb monolith adsorbed 9.34 mmol g^{-1} of methane while the powder activated

Table 4
Comparison of monolith, powder, and granular powder from different precursors.

Form (Ref. #)	Precursor	Activation Agent	Binder (wt%)	Adsorbate	BET surface area	Volumetric uptake	Gravimetric uptake
Fibers [75]	Petroleum-pitch based carbon	CO_2	N/A	Methane	1000 m^2 g^{-1}	163 V/V	e
Monolith [41]	Coffee husk	$ZnCl_2$	Polyvinyl alcohol (PVA)-5 wt%	Methane	1326 m^2 g^{-1}	130 V/V	9.34 mmol g^{-1}
Monolith [76]	Polymer-based carbide-derived carbon	Hydrogen	e	Methane	2223 m^2 g^{-1}	e	46.3 mg g^{-1}
Powder [68]	Maxsorb - chark	e	N/A	Methane	3250 m^2 g^{-1}	e	11.5 N $mmol^{-1}$ g^{-1}
Powder [77]	Coal	KOH	N/A	Methane	2599 m^2 g^{-1}	e	2.67 mmol g^{-1}

biocarbon only adsorbed 5.06 mmol g^{-1} of methane under the same high pressure of 35 atm (Table 4) [41].

While ANG requires an ambient temperature for many practical applications, decreasing the temperature while maintaining similar adsorption capacity will reduce the cost and size of the storage vessel. For example, Burchell and Rogers investigated the low–pressure adsorption of CMs for methane storage. The CMs were prepared from isotropic pitch–derived carbon fibers with phenolic resin as a binder. After the carbon and binder were uniformly mixed, it was hot pressed then carbonized. The resultant CM was then activated with carbon dioxide. The methane adsorption isotherm was performed at 500 psi. The results indicate that the CM can have an adsorption capacity of 150 V/V at 500 psi and 294 K temperature. The adsorption is very sensitive to temperature, as lowering the temperature to 285 K results in an adsorption capacity of 159 V/V (Table 1). Another unique quality of the monolith is the continuous carbon skeleton, making it electrically and thermally conductive, improving methane delivery. This particular skeletal structure allows for conductivity, when the monolith needs to be desorbed, the charge causes the gas to be released, increasing the methane delivery.

The best monolith candidate with the highest methane adsorption was run through a repetitive charge and discharge cycle for the methane adsorption, retaining 10–20% of the methane after each cycle (Fig. 13). However, delivery achieved complete desorption through the electrical desorption [14]. An example of low-pressure methane adsorption was a CM made from carbon spheres with MP and activated with KOH. These activated carbons were made from different ratios of carbon spheres, MP, and KOH pellets. Then the mixtures were pressed and placed into a tube furnace. The disc with the best results also had nitrogen doping performed on it. The best result was the disc with 75 percent of mass of carbon spheres to 25 percent carbon spheres and MP. This CM achieved decent adsorption of 3.3 mmol g^{-1} at low pressures of 100 kPa after nitrogen doping [69].

6. Problems for methane storage applications

When natural gas is being used for fuel, primarily the methane will be adsorbed and desorbed multiple times; this process produces heat that can affect the storage container. Balathanigaimani and co-workers studied the heat transfer behavior with different activated carbons by measuring temperature change during adsorption and desorption stages. The activated biocarbons studied were AC–RH derived from rice husk (AC–PKOH and AC–PH_2O, the P indicates phenol and after is the activating agent), phenol-based RP–15 and RP–20 from the company Kuraray Chemical Co., and finally Norit–B4 from Norit Co. The binders used were PVA and PVP with 90 wt% activated carbon and 5 wt% binder. The mixture was then dried and compressed to form CMs. While AC–PKOH exhibited the highest gravimetric methane adsorption of 9.76 mmol g^{-1}, RP–20 had the highest volumetric methane adsorption of 53 V/V, comparable to Norit–B4 at 52 V/V. The methane adsorption and desorption were run for ten cycles for the carbon samples and for control blanks. The temperature ranged from 27 to 30 °C for blank samples, 22–33 °C for Norit–B4, and 21–33 °C for RP–20. Despite having a homogenous surface, RP–20 had the higher isosteric heat of adsorption, resulting in a higher temperature range. The second cycle was compared to the ninth cycle for every sample to understand the heat change over time. The blank test saw low temperature results, as no adsorption or desorption was happening, and there was a slight temperature change between the second and ninth cycles. This trend was repeated for Norit–B4 with higher temperatures. However, RP–20 showed a different trend: first, there was a higher range of net temperatures, and second, the temperature slightly increased between the second and ninth cycles. These temperature changes may be due to RP–20 having a smaller average pore size of 14 Å while Norit–B4 pore size was quite large (32 Å). The speed of charge and discharge was examined and showed that the blank test had a relatively fast time for the second cycle, compared with Norit–B4 and RP–20, which had slower times. RP–20 was the slowest but was only marginally slower than Norit–B4. Overall, RP–20 had the highest volumetric methane adsorption (Table 1) and the highest temperature fluctuations, making it the best monolith for this series of experiments [1]. Another study found that the storage tank needs to be at least 110 L for enough methane storage in a vehicle. A single 40 L tank can provide a drive time of 6 min, so the 110 L tank will increase that to 16 min. While initially only 16 min, 110 L could give 2 h of driving time with an effective compression technique [8]. This study showed that work still needs to be done for methane tanks to be used in everyday vehicles.

Abdollahi and co-workers also investigated a volumetric–based apparatus to conduct cyclic operations on the CMs. The CMs were prepared from commercial M2 with 40% Novolac

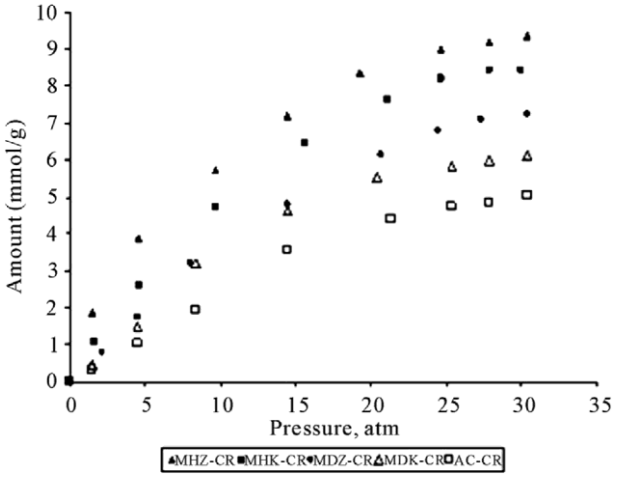

Fig. 12. Methane adsorption isotherms of activated biocarbon honeycomb coffee husks monolith. MHZ-CR, honeycomb monolith activated with $ZnCl_2$; MHK-CR honeycomb monolith activated with KOH; MDZ-CR disc monolith activated with $ZnCl_2$; MDK-CR, disc monolith activated with KOH; AC-CR activated carbon activated with $ZnCl_2$. Novel Activated Carbon Monoliths for Methane Adsorption Obtained from Coffee Husks by Liliana Giraldo, Juan Carlos Moreno-Piraj ' an is licensed under CC BY 4.0 [41].

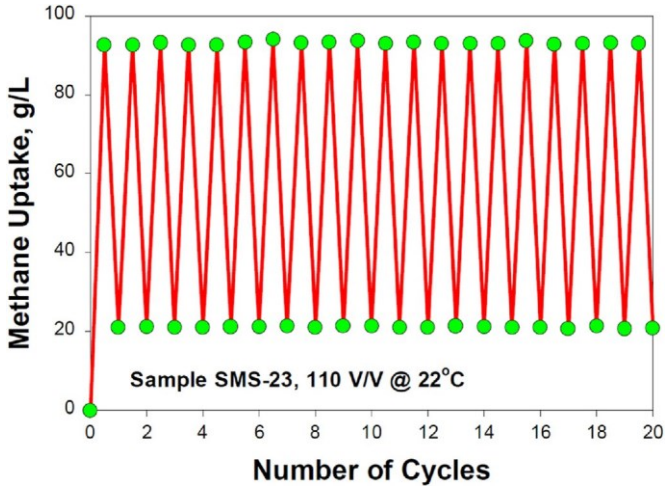

Fig. 13. Methane uptake of an ORNL storage monolith over several 20 cycles of charge and discharge SMS-23, standard monolith size-sample number. Republished with permission of SAE International, 2000; permission conveyed through Copyright Clearance Center, Inc [14].

phenolic resin as a binder. The resulting CMs showed that as absolute pressure increased, methane adsorption increased correspondingly, but the increase was less significant at higher temperatures. Fig. 14 shows the cyclic operations performed with ten adsorption and desorption runs, where the amount adsorbed and desorbed were measured. Throughout these ten cycles, the methane adsorbed slightly decreased from around 0.91 g g^{-1} to 0.87 g g^{-1}. However, the methane desorbed percentage averaged about 70% of the amount of methane adsorbed for each cycle. The lowest percent desorbed was 69.3 after eight cycles, while the highest was 71.0 for the second cycle. The efficiency was calculated from adsorption and desorption with an overall 4.4% drop in methane adsorption effectiveness and 6.2% for methane desorption effectiveness after 10 cycles. It also showed that the pores of the monolith had high retention of the methane, resulting in a high storage, although the capacity decreased gradually [15]. Additionally,

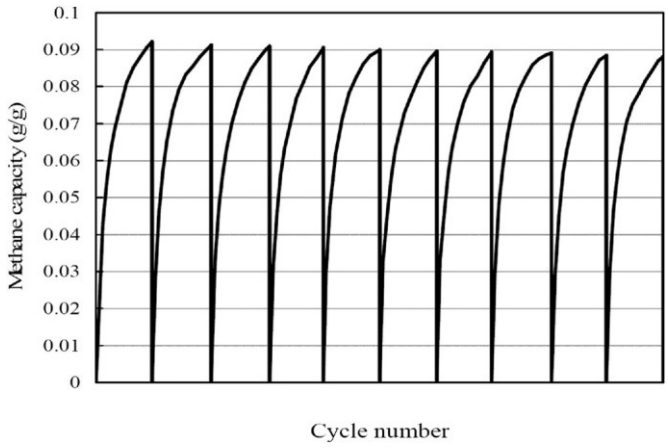

Fig. 14. Adsorption cyclic operation with pure methane for the monolith M2. Reprinted from Energy Procedia, Copyright (2017), with permission from Elsevier [15].

lower temperatures were shown to lead to a higher methane uptake [70].

Methane adsorption is widely investigated in powder or monolith form. However, reports about CM as an adsorbent in a bed storage system are rare, where more than one pellet adsorbs methane. The gravimetric loading must be in the range of 0.27–0.56 kg kg^{-1} to meet the current DOE storage target of 263 V/V volumetrically. Maxsorb III carbon powders showed 0.2 kg kg^{-1} for gravimetric loading, which correlates to a 124 V/V loading. The volumetric capacity was also analyzed after the pellet isotherm was found, which is the adsorption capacity of an individual pellet. It showed that volumetric adsorption is only part of the porosity present in the adsorbent. The set goal range of methane is 150–263 V/V to achieve this carbon storage capacity. However, this still does not consider the adsorption capacity lost during gas filling, and with that added, it lowers adsorption to 126–144 V/V. Raising the storage capacity to meet 180 V/V, the adsorption capacity of the monolith would have to be 300 V/V to meet 263 V/V actually. The capacity would have to be 373 V/V for the CM to be implemented successfully in a vehicle. This shows that the current requirements set by the DOE for methane adsorption are still too low. An adequate CM methane capacity needs to be found when the monoliths are placed in an adsorption bed to increase the amount of methane adsorbed. The above statement also shows that measuring the powder adsorption capacity is only the first step, as the gravimetric capacity of the packed bed is the most appropriate method to evaluate the capacity for practical applications [11]. In a review looking at porous carbon material for methane storage, they recognized that methane storage and meeting of the DOE parameters still requires further research within this field and that the storage materials like monoliths still need to be improved [71]. Until the methane adsorption uptake is increased, application of CM in vehicles will not be done outside of a lab setting. Therefore, novel CMs need to be developed to improve methane storage.

7. Conclusions

Activated CMs are instrumental in having ANG implemented into vehicle use. They are one kind of high-density biocarbon-based material that can be less expensive than the alternatives such as carbon fibers. Since methane is an alternative to gasoline, finding a low-cost solution for vehicle implementation is imperative. For appropriate methane uptake, optimal CM physical properties such as surface area, pore size distribution and pore volume, density, and mechanical strength must be achieved. Improved adsorption capacity in CMs can be achieved by changing the shape of the monolith, resulting in better adsorption and desorption. Therefore, a more effective binder is needed, although sometimes CMs can be fabricated with a binder-less method. By increasing the surface area and pore volume generated by adjusting the ratio of the activation agent and precursor, CMs have been prepared and have shown a high methane uptake. However, a monolith that meets all the needed parameters of large surface area, good microporosity, and high density still has not

been developed, and further research is needed. Even if the monolith methane adsorption is improved, the monolith still needs to perform in an actual application with a long life of adsorption and desorption cycles. The production of CMs as a storage vessel, with large bulk monoliths possessing high surface area and pore volume that does not sacrifice density, is still a barrier. Also, an effective way to desorb the methane from the CM into the vehicle engine without the CM being rapidly depleted remains another challenge. Finally, the method to refresh a monolith needs to be improved to return the monolith to its original adsorption capacity after repeated cycling.

Conflict of interest

The authors declare the following financial interests/personal relationships which may be considered as potential competing interests: Elizabeth Michaelis reports financial support was provided by American Chemical Society Petroleum Research Fund.

Acknowledgement

Acknowledgment is made to the Donors of the American Chemical Society Petroleum Research Fund for support of this research.

References

[1] M.S. Balathanigaimani, M.–J. Lee, W.G. Shim, J.W. Lee, H. Moon, Adsorption 14 (2008) 525–532.
[2] M. Tong, Y. Lan, Q. Yang, C. Zhong, Green Energy Environ. 3 (2018) 107–119.
[3] M. Prosniewski, A. Gillespie, E. Knight, T. Rash, D. Stalla, J. Romanos, A. Smith, J. Energy Storage 20 (2018) 357–363.
[4] D.A. Wood, C. Nwaoha, B.F. Towler, J. Nat. Gas Sci. Eng. 9 (2012) 196–208.
[5] J.L. Burger, T.M. Lovestead, T.J. Bruno, Energy Fuels 30 (2016) 2119–2126.
[6] P.K. Sahoo, M. John, B.L. Newalkar, N.V. Choudhary, K.G. Ayappa, Ind. Eng. Chem. Res. 50 (2011) 13000–13011.
[7] T. Burchell, Energia 13 (2002) 1–5.
[8] M.J. Prosniewski, T.A. Rash, E.W. Knight, A.K. Gillespie, D. Stalla, C.J. Schulz, P. Pfeifer, Adsorption 24 (2018) 541–550.
[9] A. Celzard, A. Albiniak, M. Jasienko-Halat, J.F. Mar^ech'e, G. Furdin, Carbon 43 (2005) 1990–1999.
[10] S.B. Yahia, A. Ouederni, Int. J. Chem. Eng. 3 (2012) 220–227.
[11] B.P. Prajwal, K.G. Ayappa, Adsorption 20 (2014) 769–776.
[12] S. Manzi, D. Valladares, J. Marchese, G. Zgrablich, Adsorpt. Sci. Technol. 15 (1997) 301–309.
[13] R.S. Dassanayake, C. Gunathilake, T. Jackson, M. Jaroniec, N. Abidi, Cellulose 23 (2016) 1363–1374.
[14] T. Burchell, M. Rogers, SAE Tech. Pap. 109 (2000) 2242–2246.
[15] M. Abdollahi, E.N. Lay, E. Sanjari, Energy Proc. 141 (2017) 332–338.
[16] C. Moreno-Castilla, A. P'erez-Cadenas, Materials 3 (2010) 1203–1227.
[17] R. Ubago-P'erez, F. Carrasco-Marín, D. Fair'en-Jim'enez, C. Moreno-Castilla, Microporous Mesoporous Mater. 92 (2006) 64–70.
[18] Y. Soo, N. Chada, M. Beckner, J. Romanos, J. Burress, P. Pfeifer, Bull. Am. Phys. Soc. (2013) M38.001.
[19] C. Almansa, M. Molina–Sabio, F. Rodríguez–Reinoso, Microporous Mesoporous Mater. 76 (2004) 185–191.
[20] C. Ma, J. Gong, S. Zhao, X. Liu, X. Mu, Y. Wang, X. Chen, T. Tang, Green Energy Environ. 7 (2020) 818–828.
[21] R.P. Ribeiro, T.P. Sauer, F.V. Lopes, R.F. Moreira, C.A. Grande, A.E. Rodrigues, J. Chem. Eng. Data 53 (2008) 2311–2317.
[22] A.J. Romero–Anaya, M. Kunowsky, M. Rufete–Beneite, M.A' . Lillo–R'odenas, A' . Linares–Solano, Microporous Mesoporous Mater. 284 (2019) 78–81.
[23] C. Guan, F. Su, X. Zhao, K. Wang, Separ. Purif. Technol. 64 (2008) 124–126.
[24] M. Jord'a–Beneyto, D. Lozano–Castell'o, F. Su'arez–García, D. Cazorla–Amor'os, A' . Linares–Solano, Microporous Mesoporous Mater. 112 (2008) 235–242.
[25] N. Byamba–Ochir, W.G. Shim, M.S. Balathanigaimani, H. Moon, H. Appl. Energy 190 (2017) 257–265.
[26] X. Kan, G. Zhang, Y. Luo, F. Liu, Y. Zheng, Y. Xiao, Y. Cao, C.-T. Au, S. Liang, L. Jiang, Green Energy Environ. 7 (2022) 983–995.
[27] D. Lozano–Castell'o, D. Cazorla–Amor'os, A. Linares–Solano, D.F. Quinn, Carbon 40 (2002) 2817–2825.
[28] A. Perrin, A. Celzard, J.F. Mar^ech'e, G. Furdin, Proceedings of Carbon '04 International Conference (2004) 11–16.
[29] Y. Li, X. Niu, J. Chen, Y. Feng, Ferroelectrics 562 (2020) 17–27.
[30] J. Sre'nscek–Nazzal, W. Kami'nska, B. Michalkiewicz, Z.C. Koren, Ind. Crop. Prod. 47 (2013) 153–159.
[31] Z.Q. Zhao, P.W. Xiao, L. Zhao, Y. Liu, B.H. Han, RSC Adv. 5 (2015) 73980–73988.
[32] A. Memetova, I. Tyagi, R. Rao Karri, Suhas, N. Memetov, A. Zelenin, R. Stolyarov, A. Babkin, V. Yagubov, I. Burmistrov, A. Tkachev, V. Bogoslovskiy, G. Shigabaeva, E. Galunin, Chem. Eng. J. 433 (2022) 134608.
[33] T. Kubo, H. Sakamoto, T. Fujimori, T. Itoh, T. Ohba, H. Kanoh, M. Martínez–Escandell, J.M. Ramos–Fern'andez, M. Casco, F. Rodríguez–Reinoso, K. Urita, I. Moriguchi, M. Endo, K. Kaneko, ChemSusChem 5 (2012) 2271–2277.
[34] Y. Li, W. Ma, Y. Zeng, Z. Chen, J. Wang, Q. Zhong, Electrochim. Acta 421 (2022) 140471.
[35] G. Zhai, Q. Wang, F. Liu, Z. Hu, C. Jia, D. Li, H. Xiang, M. Zhu, Green Energy Environ. (2022), https://doi.org/10.1016/j.gee.2022.04.002.
[36] G. Ning, H. Wang, X. Zhang, C. Xu, G. Chen, J. Gao, Particuology 11 (2013) 415–420.
[37] S. Xiong, Z. Wu, Z. Li, Chemosphere 287 (2022) 132418.
[38] S. Wang, J. Bai, M.T. Innocent, Q. Wang, H. Xiang, J. Tang, M. Zhu, Green Energy Environ. 7 (2021) 578–605.
[39] M.S. Balathanigaimani, W.G. Shim, J.W. Lee, H. Moon, Microporous Mesoporous Mater. 119 (2009) 47–52.
[40] W. Djeridi, A. Ouederni, A.D. Wiersum, P.L. Llewellyn, L. El Mir, Mater. Lett. 99 (2013) 184–187.
[41] L. Giraldo, J.C. Moreno–Piraj'an, Mater. Sci. Appl. (2011) 331–339, 02.
[42] J.H. Lee, Y.J. Heo, S.J. Park, Int. J. Hydrogen Energy 43 (2018) 22377–22384.
[43] Y.Q. Wang, M.Y. Zhu, Y.C. Li, M.J. Zhang, X.Y. Xue, Y.L. Shi, B. Dai, X.H. Guo, F. Yu, Green Energy Environ. 3 (2018) 172–178.
[44] J.A.F. MacDonald, D.F. Quinn, Carbon 34 (1996) 1103–1108.
[45] M. Molina–Sabio, C. Almansa, F. Rodríguez–Reinoso, Carbon 41 (2003) 2113–2119.
[46] T. Orlova, V. Shpeizman, N. Glebova, A. Nechitailov, A. Spitsyn, D. Ponomarev, A. Gutierrez-Pardo, J. Ramirez-Rico, Rev. Adv. Mater. Sci. 55 (2018) 50–60.
[47] A. Kryeziu, V. Slovak, J. Parmentier, T. Zelenka, S. Rigolet, Ind. Crop. Prod. 183 (2022) 114961.
[48] K. Adlak, R. Chandra, V.K. Vijay, K.K. Pant, J. Anal. Appl. Pyrolysis 155 (2021) 105102.
[49] D. Li, J. Zhou, Z. Zhang, Y. Tian, Y. Qiao, J. Li, L. Wen, L. Wei, Mater. Lett. 190 (2017) 127–130.
[50] A. Muto, T. Bhaskar, S. Tsuneishi, Y. Sakata, H. Ogasa, Energy Fuels 19 (2005) 251–257.
[51] J. Machnikowski, K. Kierzek, K. Torchała, Energy Fuels 26 (2012) 3697–3702.
[52] J. Machnikowski, K. Kierzek, K. Lis, H. Machnikowska, L. Czepirski, Energy Fuels 24 (2010) 3410–3414.
[53] C. Guan, L.S. Loo, K. Wang, C. Yang, Energy Convers. Manag. 52 (2011) 1258–1262.

[54] J.M. Ramos–Fern'andez, M. Martínez–Escandell, F. Rodríguez–Reinoso, Carbon 46 (2008) 384–386.
[55] T.A. Rash, A. Gillespie, B.P. Holbrook, L.H. Hiltzik, J. Romanos, Y.C. Soo, S. Sweany, P. Pfeifer, Fuel 200 (2017) 371–379.
[56] N. Bagheri, J. Abedi, Chem. Eng. Res. Des. 89 (2011) 2038–2043.
[57] D.P. Vargas, L. Giraldo, J.C. Moreno–Piraj'an, Adsorption 19 (2013) 1075–1082.
[58] R.B. Rios, F.W. Silva, A.E. Torres, D.C. Azevedo, C.L. Cavalcante, Adsorption 15 (2009) 271–277.
[59] A. Arami–Niya, W.M. Daud, F.S. Mjalli, Chem. Eng. Res. Des. 89 (2011) 657–664.
[60] L. Giraldo, J.C. Moreno–Piraj'an, Adsorpt. Sci. Technol. 27 (2009) 255–265.
[61] J.P. Marco–Lozar, M. Kunowsky, F. Su'arez–García, J.D. Carruthers, A. Linares–Solano, Energy Environ. Sci. 5 (2012) 9833–9842.
[62] M.J. Prauchner, K. Sapag, F. Rodríguez–Reinoso, Carbon 110 (2016) 138–147.
[63] M. Kunowsky, J.P. Marco–Lozar, F. Su'arez–García, A'. Linares–Solano, J.D. Carruthers, Int. J. Appl. Ceram. Technol. 12 (2015) E121–E126.
[64] F. Rodríguez–Reinoso, Y. Nakagawa, J. Silvestre–Albero, J.M. Ju'arez–Gal'an, M. Molina–Sabio, Microporous Mesoporous Mater. 115 (2008) 603–608.
[65] A.A.G. Blanco, J.C.A. de Oliveira, R. L'opez, J.C. Moreno–Piraj'an, L. Giraldo, G. Zgrablich, K. Sapag, Colloids Surf. A Physicochem. Eng. Asp. 357 (2010) 74–83.
[66] D. Cao, X. Zhang, J. Chen, W. Wang, J. Yun, J. Phys. Chem. B 107 (2003) 13286–13292.
[67] M. Kwiatkowski, D.P. Vargas Delgadillo, J. Mater. Res. Technol. 8 (2019) 4457–4463.
[68] S. Himeno, T. Komatsu, S. Fujita, J. Chem. Eng. Data 50 (2005) 369–376.
[69] S. Gao, L. Ge, B.S. Villacorta, T.E. Rufford, Z. Zhu, Ind. Eng. Chem. Res. 58 (2019) 4957–4969.
[70] E.M. Strizhenov, A.A. Zherdev, R.V. Petrochenko, D.A. Zhidkov, R.A. Kuznetsov, S.S. Chugaev, A.A. Podchufarov, D.V. Kurnasov, Chem. Pet. Eng. 52 (2017) 838–845.
[71] A. Memetova, I. Tyagi, R. Rao Karri, V. Kumar, K. Tyagi, Suhas, N. Memetov, A. Zelenin, T. Pasko, A. Gerasimova, D. Tarov, M. Hadi Dehghani, K. Singh, Chem. Eng. J. 446 (2022) 137373.
[72] C. Solar, F. Sardella, C. Deiana, R.M. Lago, A. Vallone, K. Sapag, Mater. Res. 11 (2008) 409–414.
[73] Y. Wang, M. Hashim, C. Ercan, A. Khawajah, R. Othman, In 21st Annual Saudi–Japan Symposium (2011).
[74] B.R. Alfadlil, G.P. Knowles, M.R.N. Parsa, R.R.D. Subagyono, Daniel, A.L. Chaffee, J. Phys. Conf. Ser. 1277 (2019) 012024.
[75] J. Alca~niz–Monge, M.A. De La Casa–Lillo, D. Cazorla–Amor'os, A. Linares–Solano, Carbon 35 (1997) 291–297.
[76] M. Oschatz, L. Borchardt, I. Senkovska, N. Klein, M. Leistner, S. Kaskel, Carbon 56 (2013) 139–145.
[77] A. Toprak, T. Kopac, Int. J. Chem. React. Eng. 15 (2018) 20180146.